Journal of Applied Electrochemistry **34**: 409–415, 2004.

Development of LSM/YSZ composite cathode for anode-supported solid oxide fuel cells

Y.J. LENG, S.H. CHAN*, K.A. KHOR and S.P. JIANG
Fuel Cell Strategic Research Programme, School of Mechanical and Production Engineering, Nanyang Technological University, 50 Nanyang Avenue, Singapore 639798
*(*author for correspondence, e-mail: MSHCHAN@ntu.edu.sg)*

Received 28 January 2003; accepted in revised form 4 November 2003

Key words: cathodic treatment, composite cathode, electrolyte surface grinding, LSM non-stoichiometry, solid oxide fuel cell

Abstract

This paper presents the effect of (La,Sr)MnO_3 (LSM) stoichiometry on the polarization behaviour of LSM/Y_2O_3-ZrO_2 (YSZ) composite cathodes. The composite cathode made of A-site deficient $(La_{0.85}Sr_{0.15})_{0.9}MnO_3$ (LSM-B) showed much lower electrode interfacial resistance and overpotential losses than that made of stoichiometric $(La_{0.85}Sr_{0.15})_{1.0}MnO_3$ (LSM-A). The much poorer performance of the latter is believed to be due to the formation of resistive substances such as $La_2Zr_2O_7/SrZrO_3$ between LSM and YSZ phases in the composite electrode. A slight A-site deficiency (~0.1) was effective in inhibiting the formation of these resistive substances. A power density of ~1 W cm^{-2} at 800 °C was achieved with an anode-supported cell using an LSM-B/YSZ composite cathode. In addition, the effects of cathodic current treatment and electrolyte surface grinding on the performance of composite cathodes were also studied.

1. Introduction

Electrode-supported, in particular anode-supported, solid oxide fuel cells (SOFCs) with thin film yttria-stabilized zirconia (YSZ) electrolyte have attracted great interest recently due to their better performance than electrolyte-supported SOFCs operating at intermediate temperatures (600–800 °C) [1–5]. Because of the thin electrolyte, and hence reduced ohmic resistance, used in the electrode-supported fuel cell and the fact that the anode resistance is in general very low in SOFC, it is logical to focus effort on the cathode optimization. Ralph et al. [6] showed that, at operating temperatures above 650 °C, the ohmic losses associated with YSZ thin film electrolyte is insignificant, while the cathode polarization is often the limiting factor in SOFC performance operating at intermediate temperatures.

$La_{1-x}Sr_xMnO_3$ perovskite (LSM) is one of the most promising materials for cathodes in high temperature SOFCs because of its high thermal and chemical stability, high electrochemical activity and relatively good compatibility with YSZ [7, 8]. However, its low ionic conductivity and high activation energy limit its application in intermediate-temperature SOFCs. One commonly used method to improve the LSM cathode performance is to add some ionically conducting material such as YSZ to form a composite cathode [9–12]. Some evidence showed that the performance of LSM/YSZ composite cathodes is strongly dependent on the properties of the materials, processing techniques and composition of the materials [9–11]. In addition, the polarization and stability of pure LSM electrodes are critically dependent on the stoichiometry composition of LSM material [13,14]. In this study, we extended our investigation into the effect of the LSM stoichiometry on the performance of LSM/YSZ composite cathodes. In addition, the effects of cathodic current treatment and electrolyte surface grinding on the polarization behaviour of LSM/YSZ cathodes were also investigated.

2. Experimental details

The electrolyte was prepared from 8 mol % Y_2O_3–ZrO_2 (Tosoh, Japan) by a conventional ceramic processing technique (i.e., mixing and uniaxially pressing (100 Mpa)), followed by sintering at 1500 °C for 4 h. The electrolyte thickness was ~0.90 mm for as-fired samples and it reduced to ~0.75 mm after grinding with sandpaper (400 mesh). LSM powder was purchased from Nextech, USA with composition of $La_{0.85}Sr_{0.15}$-MnO_3, which is A-site stoichiometry (denoted as LSM-A). To make A-site non-stoichiometry, that is, $(La_{0.85}$-$Sr_{0.15})_{0.9}MnO_3$ (denoted as LSM-B), LSM-A was mixed with the appropriate amount of $MnCO_3$ and calcined at 900 °C for 1 h. LSM/YSZ with composition of 50 wt %

LSM (LSM-A or LSM-B) and 50 wt % YSZ was prepared by mixing LSM with YSZ powders, followed by ball-milling for 12 h. Our previous simulation study showed that mixing the LSM with YSZ powders in a one-to-one volume ratio with similar particle size could likely achieve the lowest composite cathode overpotential [15]. Based on this, LSM/YSZ ink was prepared by mixing the powders with polyethylene glycol using a mortar and a pestle. The ink was then applied to the YSZ electrolyte substrate by screen-printing method and fired at 1150 °C for 2 h. The electrode was ~10 μm in thickness and 0.50 cm^2 in area. The LSM-A/$MnCO_3$/YSZ electrode was prepared by adding $MnCO_3$ to the LSM-A/YSZ composite in a mass ratio of 50:2.5:50. LSM-A/$MnCO_3$/YSZ electrode was then introduced to YSZ electrolyte in a similar way as above. A current collector was added to the cathode by painting a layer of Pt paste (Ferro Corporation, USA) on its surface, then fired at 1100 °C for 15 min. Pt paste was also painted onto the other side of the YSZ electrolyte disc to serve as the counter and reference electrode.

Electrochemical measurements were conducted using Autolab PG30/FRA system (Eco Chimie, The Netherlands). Electrode characteristics of composite cathodes were studied using a galvanostatic method and electrochemical impedance spectroscopy (EIS). The polarization measurement was carried out at a constant cathodic current of 200 mA cm^{-2} at 800 °C in air and the cathodic polarization potential ($E_{cathode}$) was recorded. The polarization was interrupted from time to time for the EIS measurement. The impedance was measured in the frequency range 100 kHz – 0.1 Hz with a signal amplitude of 10 mV at open-circuit. The electrode was equilibrated at open circuit for about 10 min prior to the EIS measurement. The electrode interfacial (polarization) resistance (R_E) was directly obtained from the difference between the low and high frequency intercepts on the impedance real axis. Overpotential (η) and electrode ohmic resistance (R_{ohm}) between the cathode and the Pt reference electrode were calculated using the data extracted from the galvanostatic and impedance spectroscopy measurements.

An anode-supported SOFC was fabricated with Ni-YSZ (50:50 wt %) anode support (~0.75 mm thick), thin film YSZ electrolyte (18 μm thick) and LSM-B/YSZ cathode (10–20 μm thick). The techniques used for fabricating the anode support, YSZ electrolyte and cathode were die pressing, spray coating and screen-printing, respectively. The cell performance was measured using an in-house built SOFC test station at 800 °C. Details of the cell fabrication and measurement of cell performance have been reported previously [16].

Scanning electron microscopy (SEM, Jeol 6500) was used to examine the morphology and microstructure of the cathodes, YSZ electrolyte and anode-supported cell. The phases in the LSM and LSM/YSZ cathodes were examined with an X-ray diffractometer (XRD) using CuK_α radiation.

3. Results and discussion

3.1. *XRD and SEM examination*

Figure 1 shows XRD diagrams of Nextech $La_{0.85}Sr_{0.15}MnO_3$ powder (LSM-A) and as prepared $(La_{0.85}Sr_{0.15})_{0.9}MnO_3$ powder (LSM-B). Identical XRD patterns confirmed the single perovskite phase for both powders. This indicates that after calcining $MnCO_3$/LSM-A mixture at 900 °C for 1 h, A-site substoichiometric powder (LSM-B) has successfully been obtained with manganese being incorporated into the LSM perovskite structure.

Figure 2 shows the XRD diagram of disc specimens made of LSM-A/YSZ and LSM-B/YSZ composite powders sintered at 1150 °C for 4 h. In both cases, the primary phases are LSM perovskite and YSZ cubic phases. However, different to that of LSM-B/YSZ, there are two additional unknown peaks at $2\theta = 42.5$ and 71.4° detected for the pellets made of LSM-A and YSZ mixture (Figure 2(b)), which we could not identify at this stage. As the XRD curves associated with $La_2Zr_2O_7$ and $SrZrO_3$ overlap with those of LSM perovskite structure [17], the presence of minor $La_2Zr_2O_7$ and $SrZrO_3$ phases between LSM-A and YSZ may not be detectable by XRD. Murry and Barnett were also unable to identify the existence of $La_2Zr_2O_7/SrZrO_3$ phase in their $La_{0.8}Sr_{0.2}MnO_3$-YSZ (50:50 wt %) sample sintered at 1150 °C for 2 h using XRD [18]. However, it is well known that stoichiometric LSM has a tendency to react with YSZ to form lanthanum zirconate ($La_2Zr_2O_7$), a resistive substance at temperatures as low as 1000 °C [13,14,19,20]. Thus, it is quite possible that there could be a thin resistive $La_2Zr_2O_7$ layer formed between LSM-A and YSZ grains in the LSM-A/YSZ electrodes.

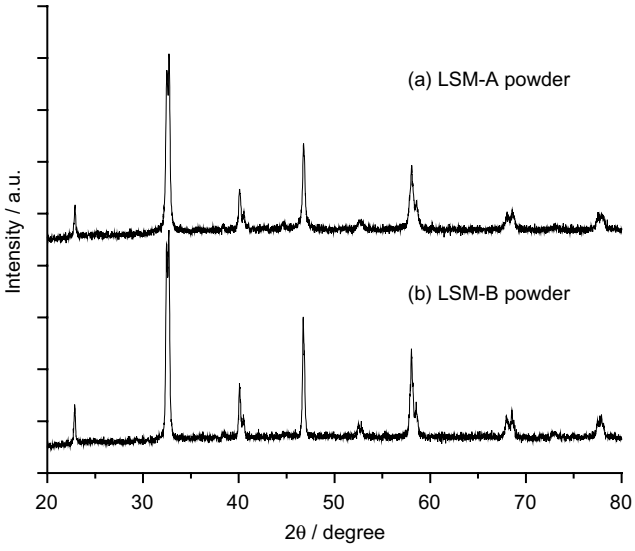

Fig. 1. X-ray diffraction diagrams of (a) commercial LSM powder (LSM-A) and (b) modified LSM powder (LSM-B).

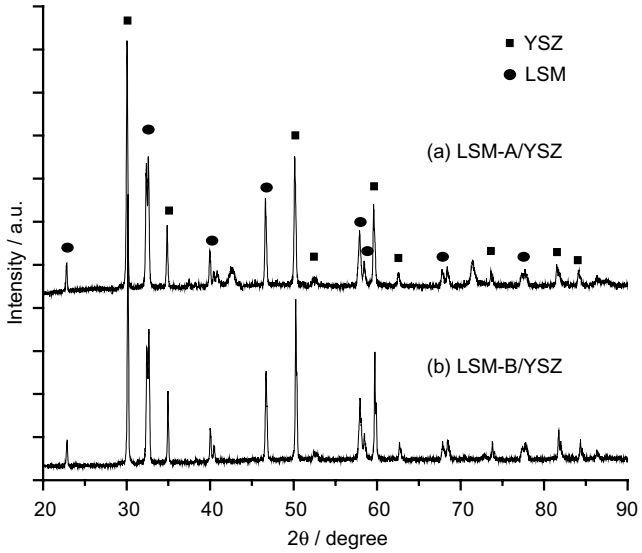

Fig. 2. X-ray diffraction diagrams of the pellets made of (a) LSM-A/YSZ (50:50 wt %) mixture and (b) LSM-B/YSZ (50:50 wt %) mixture after being sintered at 1150 °C for 4 h.

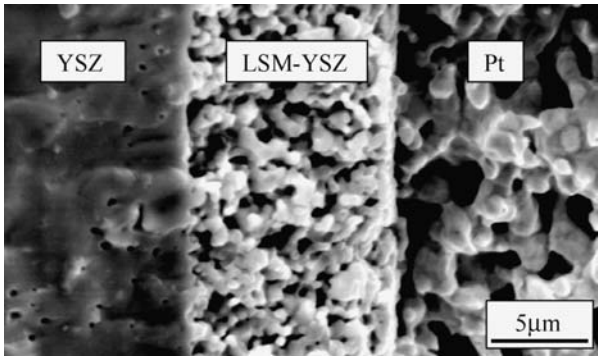

Fig. 3. SEM picture of the fractured cross section of LSM/YSZ composite cathode, showing a typical composite cathode sintered at 1150 °C for 2 h on YSZ electrolyte.

Figure 3 shows the SEM micrograph showing the cross sectional view of an LSM-YSZ cathode (~10 μm thick) fabricated on the YSZ electrolyte. The LSM and YSZ grains appear to have sintered well with each other and bonded well at the LSM-YSZ/YSZ interface. The platinum current collector with a thickness of ~20 μm is also bonded well with the cathode. In addition, there is sufficient porosity for gas diffusion in the platinum layer.

3.2. *Polarization performance of LSM/YSZ cathodes*

Figure 4 shows the impedance and polarization responses of an LSM-A/YSZ cathode under a cathodic current density of 200 mA cm^{-2} at 800 °C in air. Before cathodic current was applied, the impedance response was characterized by a large and depressed arc and the initial electrode interfacial resistance (R_E) was 6.6 Ω cm^2. After 4 h of cathodic current, R_E was reduced to 4.5 Ω cm^2, ~32% lower than the initial R_E of 6.6 Ω cm^2

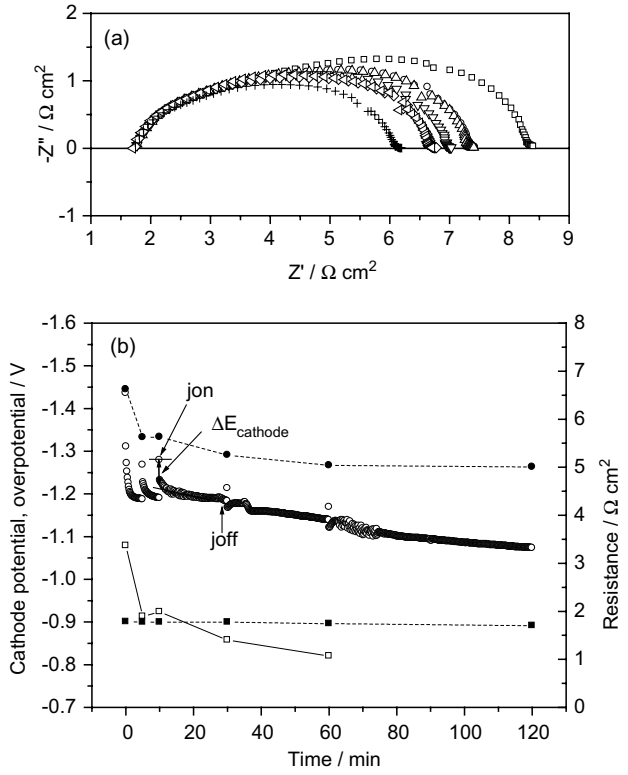

Fig. 4. Initial impedance and polarization response of a LSM-A/YSZ cathodes under a cathodic current of 200 mA cm^{-2} at 800 °C in air. (a) Impedance for different cathodic current passage time: (□) 0, (○) 5, (△) 10, (▽) 30, (◇) 60, (◁) 120 and (+) 240 min. (b) Polarization response: (○) cathode potential $E_{cathode}$, (–□–) cathode overpotential η_c, (- -■- -) ohmic resistance R_{ohm}, (- -●- -) interfacial resistance R_E.

(Figure 4(a)). Further cathodic current treatment had little effect on R_E. The effect of the cathodic current was mainly on the electrode impedance at low frequencies. The polarization behaviour of O_2 reduction on LSM-A/YSZ cathodes at 200 mA cm^{-2} was similar to the impedance responses. Initial overpotential loss (η) at 200 mA cm^{-2} was 1080 mV for the cathode before cathodic current passage. After 1 h of cathodic treatment at 200 mA cm^{-2}, η was reduced to ~820 mV, a reduction of ~24%. Despite the significant change in the polarization potential, the electrode ohmic resistance (R_{ohm}) remained more or less constant, indicating that the decrease in $E_{cathode}$ was purely due to the reduction of cathodic overpotential (η). The reduction in η and R_E confirmed the activation effect of cathodic treatment on the initial polarization behaviour of the LSM-A/YSZ composite cathode, similar to that on pure LSM cathodes [13, 21].

A similar activation effect of cathodic treatment was observed for LSM-B/YSZ cathodes. Figure 5 shows the initial impedance and polarization responses of an LSM-B/YSZ cathode under the same cathodic current treatment conditions. After 4 h of current passage, R_E was reduced to 0.50 Ω cm^2, ~30% lower than the initial R_E of 0.71 Ω cm^2. Similar to the impedance response, after 1 h of treatment, η at 200 mA cm^{-2} was reduced to ~120 mV, about 16% lower than the initial η of

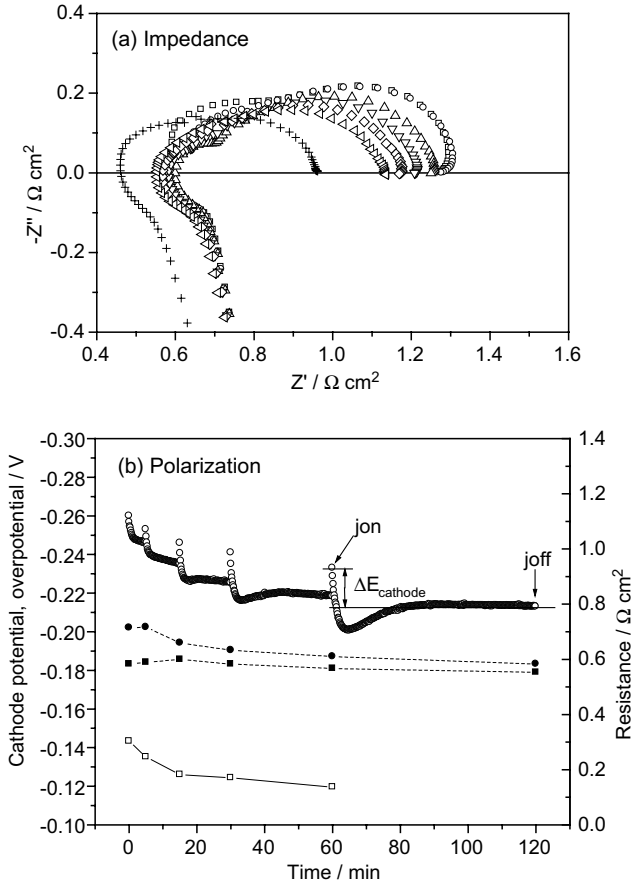

Fig. 5. Initial impedance and polarization response of a LSM-B/YSZ cathode under a cathodic current of 200 mA cm^{-2} at 800 °C in air. (a) Impedance for different cathodic current passage time: (□) 0, (○) 5, (△) 10, (▽) 30, (◇) 60, (◁) 120 and (+) 240 min. (b) Polarization response: (○) cathode potential $E_{cathode}$, (–□–) cathode overpotential η_c, (--■--) ohmic resistance R_{ohm}, (--●--) interfacial resistance R_E.

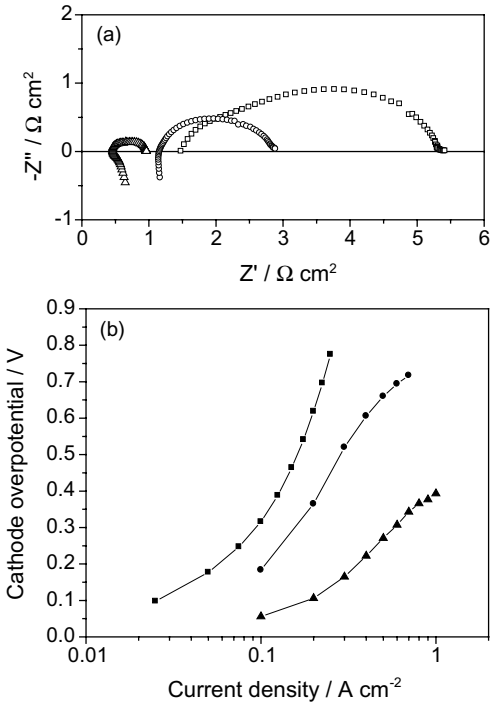

Fig. 6. (a) Impedance and (b) polarization curves of composite cathodes measured at 800 °C in air. (□, --■--) LSM-A/YSZ (50:50 wt %), (○, --●--) LSM-A/$MnCO_3$/YSZ (50:2.5:50 by weight), (△, –▲–) LSM-B/YSZ (50:50 wt %).

~143 mV. However, R_E and η of the LSM-B/YSZ cathode were much smaller than those of the LSM-A/YSZ cathode. For O_2 reduction on the LSM-B/YSZ cathode, the initial R_E was 0.71 Ω cm^2; much smaller than the initial R_E of 6.6 Ω cm^2 on LSM-A/YSZ cathode. Nevertheless, two overlapping semicircles were clearly observed for both LSM-A/YSZ and LSM-B/YSZ cathodes in the high frequency and low frequency ranges, respectively. This indicates the existence of at least two different electrode processes corresponding to high and low frequencies [10, 22].

Figure 6 shows the impedance and polarization curves of LSM-A/YSZ, LSM-A/$MnCO_3$/YSZ and LSM-B/YSZ cathodes at 800 °C in air. Impedance was measured under open circuit conditions. The electrodes were stabilized with cathodic treatment at 200 mA cm^{-2} and 800 °C for 4 h. The electrode interfacial resistance (R_E) of LSM-B/YSZ cathode was 0.5 Ω cm^2, three times smaller than 1.7 Ω cm^2 of the LSM-A/$MnCO_3$/YSZ cathode and eight times smaller than 3.94 Ω cm^2 of the LSM-A/YSZ cathode. Similarly, the non-stoichiometric LSM-B/YSZ cathode showed much better performance as compared to that of the stoichiometric LSM-A/YSZ cathode. For example, at 200 mA cm^{-2}, the overpotential of oxygen reduction on LSM-B/YSZ was 106 mV, much smaller than the 365 mV measured on the LSM-A/$MnCO_3$/YSZ cathode and the 619 mV measured on the LSM-A/YSZ cathode. The electrode ohmic resistance of the LSM-A/YSZ, LSM-A/$MnCO_3$/YSZ and LSM-B/YSZ cathodes at 800 °C in air was 1.47, 1.17 and 0.46 Ω cm^2, respectively. The thickness of the electrolyte discs used was similar, in the range of 0.90 ± 0.02 mm.

The significant difference in the polarization behaviour among LSM-A/YSZ, LSM-A/$MnCO_3$/YSZ and LSM-B/YSZ cathodes for O_2 reduction demonstrates the importance of the LSM stoichiometry in determining the performance of composite cathodes. LSM stoichiometry plays a critical role in the LSM material stability and the formation of lanthanum zirconate ($La_2Zr_2O_7$) resistive phase between LSM and YSZ [8, 13, 23]. An A-site non-stoichiometric LSM is effective in inhibiting the formation of $La_2Zr_2O_7$ and greatly improves the stability and polarization performance [13, 14]. Though it was impossible to detect the $La_2Zr_2O_7$ and $SrZrO_3$ phases in the LSM-A/YSZ/YSZ by XRD, the much higher polarization losses, electrode interfacial resistance (R_E) and electrode ohmic resistance (R_{ohm}) of LSM-A/YSZ cathode are most likely due to the formation of these resistive substances, which is similar to the interfacial reactions between stoichiometric LSM and YSZ powders [13, 14, 19, 20, 23]. It is believed that the resistive $La_2Zr_2O_7$ and/or $SrZrO_3$ phases formed block the transfer path of oxygen ions at the three-phase

boundary (TPB) and active sites for the oxygen dissociative adsorption and/or the surface diffusion of oxygen species, leading to significant reduction in LSM-A/YSZ cathode performance. This conclusion is also supported by the decreased polarization losses, R_E and R_{ohm} for O_2 reduction on LSM-A/$MnCO_3$/YSZ and LSM-B/YSZ cathodes as A-site non-stoichiometry LSM or Mn excess in the LSM/YSZ electrode would suppress the formation of resistive substances [13, 14, 23]. Among all electrodes studied, the LSM-B/YSZ cathode showed the best performance. This indicates that A-site non-stoichiometry LSM is more effective in inhibiting $La_2Zr_2O_7$ phase formation than Mn excess in the LSM-A/$MnCO_3$/YSZ electrode.

After cathodic treatment at 200 mA cm^{-2} and 800 °C for 4 h, the electrode interfacial resistance and overpotential of LSM-A/YSZ cathode were still much higher than that of LSM-B/YSZ. In addition, the change in electrode ohmic resistance of the LSM-A/YSZ electrode was negligible after cathodic treatment. These results indicate that the activation effect of cathodic treatment on the initial polarization performance of the LSM-A/YSZ cathode may not due to the break up of resistance substances. In fact, a similar activation effect of cathodic treatment on the initial polarization performance of LSM-B/YSZ cathode was also observed. It is not clear, at this stage, why the current treatment is less effective in LSM/YSZ composite electrodes than in pure LSM electrodes [13]. Nevertheless, the effect of cathodic treatment on polarization behaviour of the LSM/YSZ composite electrodes could be due to the microstructural improvement, reduction in the passivation species such as SrO on the LSM surface and generation of oxygen vacancies, similar to that on pure LSM electrodes [13, 21, 24, 25].

3.3. *Effect of YSZ surface grinding*

Figure 7 shows the Nyquist and Bode impedance plots at 800 °C and 750 °C in air for an LSM-B/YSZ cathode on YSZ electrolyte with and without surface grinding. In this Figure, symbols are the measured data and lines are the fitted results using the equivalent circuit in Figure 7(a). In the equivalent circuit, L is an inductor, R_s is ohmic resistance, RH and RL are electrode resistance of high-frequency and low-frequency arcs, and QH and QL are constant phase elements (CPE) of high-frequency and low-frequency arcs, respectively.

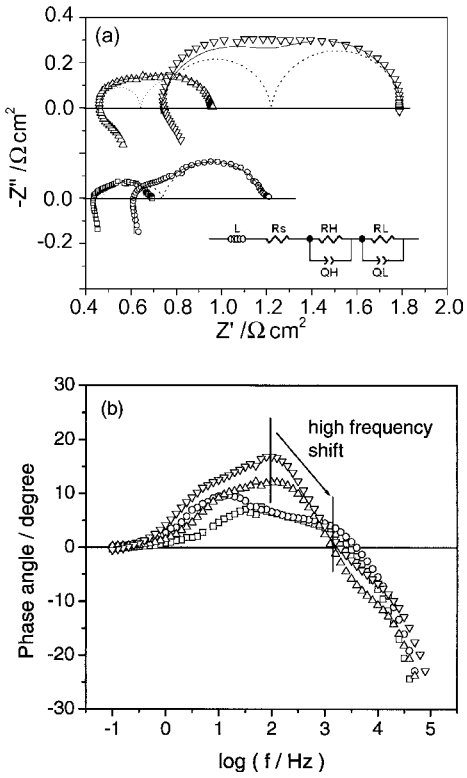

Fig. 7. (a) Nyquist and (b) Bode plots of impedance measured in air and under OCV of an LSM-B/YSZ composite cathode with and without YSZ electrolyte surface treatment: (□) 800 °C, on ground surface; (○) 750 °C, on ground surface; (△) 800 °C, on as-sintered surface; (▽) 750 °C, on as-sintered surface. Also shown in Nyquist plot (a) are the corresponding equivalent circuit and the fitting curves at 750 °C.

The observed impedence spectrum for O_2 reduction on LSM-B/YSZ can be resolved into two impedance arcs and the fitting of the observed data with the equivalent circuit yields two time constants. The fitted results are shown in Table 1. After surface grinding, the size of the high frequency arc decreased significantly, while the change in the low frequency arc was very small. For example, at 800 °C the electrode interfacial resistance of the high frequency arc after grinding was 0.034 Ω cm^2, six times smaller than the 0.187 Ω cm^2 before grinding. On the other hand, the electrode interfacial resistance of the low frequency arc after grinding decreased slightly from 0.313 Ω cm^2 before grinding to 0.223 Ω cm^2. There was also a significant change in the time constant for the high frequency arc after electrolyte surface grinding, but the change in the time constant for the

Table 1. Impedance parameters for O_2 reduction on the LSM-B/YSZ composite cathode on ground and as-sintered YSZ electrolyte surface

YSZ surface	Temperature /°C	L /Hy	R_s /Ω cm^2	High frequency arc				Low frequency arc			
				RH /Ω cm^2	QH /F cm^{-2} s^n	n	RQ τ_H/ms	RL /Ω cm^2	QL /F cm^{-2} s^n	n	RQ τ_L/ms
Ground	800	1.96×10^{-6}	0.436	0.034	6.28×10^{-3}	1.00	0.21	0.223	2.75×10^{-2}	0.72	6.1
Ground	750	2.07×10^{-6}	0.613	0.124	2.84×10^{-3}	0.87	0.35	0.459	3.71×10^{-2}	0.77	17.0
As-sintered	800	5.46×10^{-6}	0.454	0.187	6.40×10^{-3}	0.98	1.20	0.313	4.50×10^{-2}	0.89	14.1
As-sintered	750	3.98×10^{-6}	0.730	0.490	4.01×10^{-3}	0.92	1.96	0.583	4.91×10^{-2}	0.91	28.6

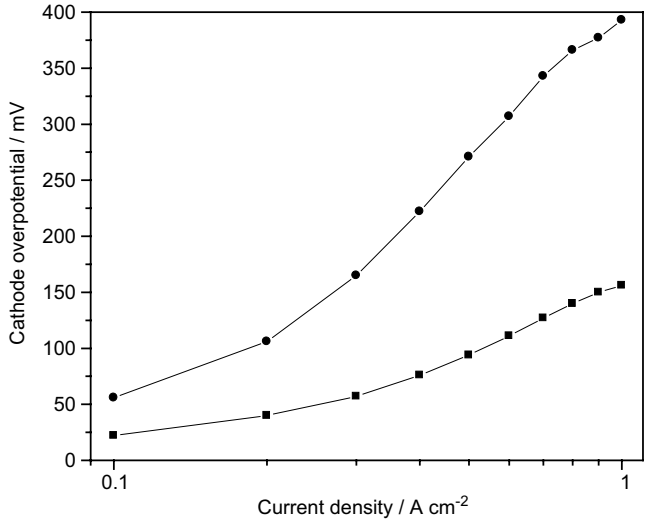

Fig. 8. Polarization curve of an LSM-B/YSZ composite cathode on ground and on as-sintered YSZ electrolyte surface measured at 800 °C in air: (–■–) on ground YSZ surface, (–●–) on as-sintered YSZ surface.

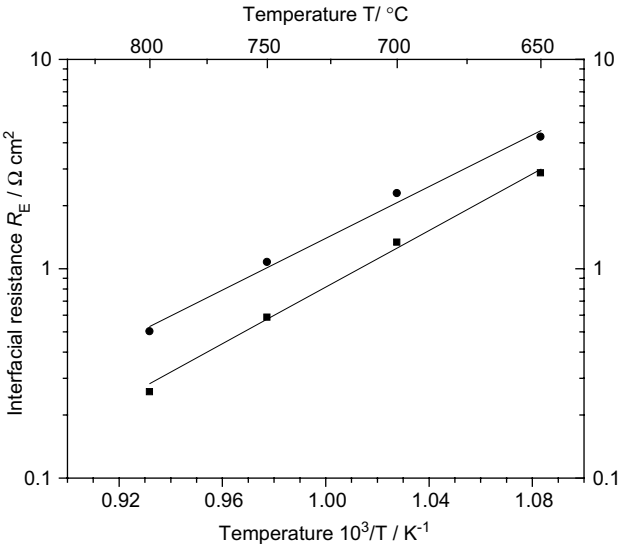

Fig. 9. Activation plots of interfacial polarization resistance of LSM-B/YSZ composite cathode on ground and on as-sintered YSZ electrolyte surface measured in air: (■) on ground YSZ surface, E_a=1.35 eV; (●) on as-sintered YSZ surface, E_a=1.22 eV.

corresponding low frequency arc was relatively small (Table 1). This is also indicated by a high frequency shift of phase angle corresponding the high frequency arc. SEM examination of the YSZ surface showed that the electrolyte surface after grinding was much rougher than the as-sintered electrolyte surface. Thus, surface grinding has significantly increased the contact area between the LSM/YSZ electrode and YSZ electrolyte, promoting oxygen ion transfer from the three phase boundaries to the YSZ electrolyte [22]. This again confirms that the reaction steps associated with the high frequency arc for O_2 reduction on LSM/YSZ are most likely related to oxygen ion transfer between the LSM and YSZ phases [10], consistent with that observed on pure LSM [22]. The total electrode interfacial resistance of the LSM-B/YSZ electrode on ground YSZ electrolyte was 0.26 Ω cm^2 as compared to 0.50 Ω cm^2 observed on as-sintered YSZ electrolyte.

Figure 8 shows the polarization curve of an LSM-B/YSZ cathode on YSZ electrolyte with and without surface grinding at 800 °C in air. The polarization behaviour of LSM-B/YSZ cathode on ground YSZ electrolyte was significantly improved as compared to that on as-sintered YSZ. For example, η at 500 mA cm^{-2} was 94 mV for O_2 reduction on LSM-B/YSZ on a ground YSZ surface, much lower than 271 mV for the electrode on as-sintered YSZ. The poor performance of as-sintered YSZ was likely due to its smooth surface with poor contact between electrode and electrolyte. In addition, impurities such as silica and alumina may segregate to the surface after sintering, increasing interfacial resistance. Therefore, surface treatment such as grinding can remove the surface impurities and roughen the electrolyte surface, increasing the contact points between electrolyte and cathode and thus increasing the reaction sites for oxygen ions to migrate from the cathode to the electrolyte. However, it seems that surface grinding has little effect on the activation process of the O_2 reduction reaction on LSM-B/YSZ, as shown in Figure 9. The activation energy for oxygen reduction on LSM-B/YSZ on YSZ with surface grinding was 1.35 eV, close to 1.22 eV for the reaction on YSZ without grinding.

3.4. *Performance of anode-supported solid oxide fuel cell with LSM-B/YSZ cathode*

Figure 10 shows the open circuit voltage (OCV) and the cell performance at 800 °C. The cell was made of ~18 μm thick YSZ electrolyte, Ni/YSZ anode (~0.75 mm thick) and LSM-B/YSZ cathode (10–20 μm thick). The OCV was 1.06 V (very close to the theoretical value), which indicates that the thin film YSZ electrolyte

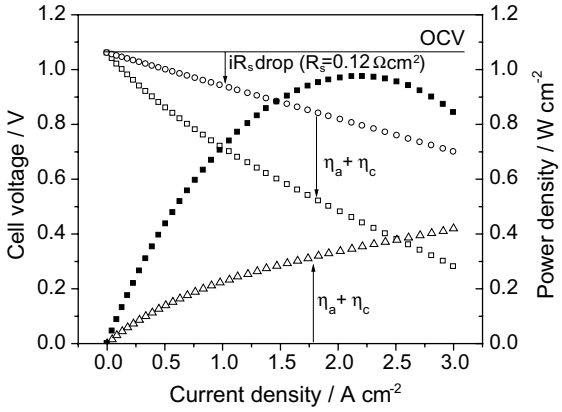

Fig. 10. Cell voltage and power density against current density tested at 800 °C for an anode-supported solid oxide fuel cell with 18 μm thin film YSZ electrolyte and LSM-B/YSZ composite cathode: (■) power density, (□) cell voltage, (○) OCV minus ohmic drop, (△) electrode overpotential.

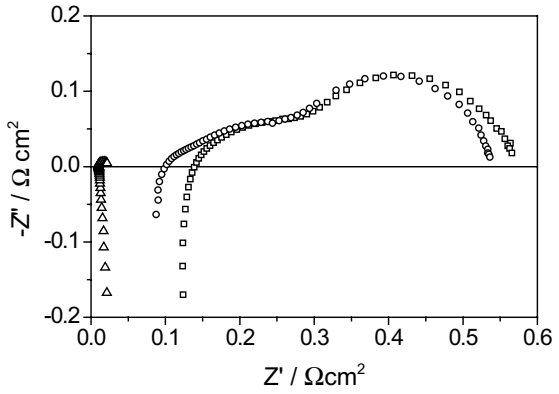

Fig. 11. Impedance of anode, cathode and cell of an anode-supported solid oxide fuel cell with thin film YSZ electrolyte and LSM-B/YSZ composite cathode measured at 800 °C and OCV: (□) cell, (○) cathode, (△) anode.

has achieved a dense structure. The cell ohmic resistance was 0.12 Ω cm^2, and the maximum power density was 0.98 W cm^{-2} at 800 °C. Figure 11 shows the impedance curves of anode, cathode and cell, measured with a Pt reference electrode located on the cathode at 800 °C. It appears that cell polarization was mainly due to loss on the cathode side. However, the extremely low polarization losses for the H_2 oxidation reaction on the anode may raise the question on the reliability of reference electrodes in anode-supported cells [26].

4. Conclusion

The effect of LSM stoichiometry and Mn excess on the polarization performance of LSM/Y_2O_3-ZrO_2 (YSZ) cathodes was studied. The cathode made of non-stoichiometric LSM-B showed much lower electrode interfacial resistance and polarization losses than that made of stoichiometric LSM-A. The much poorer performance of the LSM-A/YSZ electrode was most likely due to the formation of resistive substances such as $La_2Zr_2O_7$/$SrZrO_3$ between LSM and YSZ phases in the electrode. A slight A-site deficiency (~0.1) or Mn excess in stoichiometry LSM-A was effective in inhibiting the formation of such resistive substances. A power density of about 1 W cm^{-2} at 800 °C was achieved on an anode-supported cell using an LSM-B/YSZ cathode with an electrolyte thickness of about 18 μm.

The effects of cathodic treatment and electrolyte surface grinding on the performance of LSM/YSZ cathodes were also investigated. The cathodic treatment had an activation effect on the initial polarization performance of both stoichiometric LSM-A/YSZ and non-stoichiometric LSM-B/YSZ cathodes. This indicates that the activation effect of cathodic current treatment may not be related to the break up of passive layers such as lanthanum zirconate on the LSM surface. Surface grinding of YSZ electrolyte had a significant effect on the performance of LSM/YSZ electrodes.

References

1. J.W. Kim, A.V. Virkar, K.Z. Fung, K. Mehta and S.C. Singhal, *J. Electrochem. Soc.* **146** (1999) 69.
2. Y. Jiang and A.V. Virkar, *J. Electrochem. Soc.* **148** (2001) A706.
3. C. Wang, W.L. Worrell, S. Park, J.M. Vohs and R.J. Gorte, *J. Electrochem. Soc.* **148** (2001) A864.
4. S. de Souza, S.J. Visco and L.C. de Jonghe, *J. Electrochem. Soc.* **144** (1997) L35–37.
5. T. Tsai and S.A. Barnett, *Solid State Ionics* **98** (1997) 207.
6. J.M. Ralph, A.C. Schoeler and M. Krumpelt, *J. Mater. Sci.* **36** (2001) 1161.
7. N.Q. Minh, *J. Am. Ceram. Soc.* **76** (1993) 563.
8. S.P. Jiang, *J. Power Sources*, in press.
9. T. Tsai and S.A. Barnett, *Solid State Ionics* **98** (1997) 191.
10. J.D. Kim, G.D. Kim, J.W. Moon, Y.I. Park, W.H. Lee, K. Kobayashi, M. Nagai and C.E. Kim, *Solid State Ionics* **143** (2001) 379.
11. M.J. Joergensen, S. Primdahl, C. Bagger and M. Mogensen, *Solid State Ionics* **139** (2001) 1.
12. S.P. Jiang, Y.J. Leng, S.H. Chan and K.A. Khor, *Electrochem. Solid-State Lett.* **6** (2003) A67.
13. S.P. Jiang, J.G. Love, J.P. Zhang, M. Hoang, Y. Ramprakash, A.E. Hughes and S.P.S. Badwal, *Solid State Ionics* **121** (1999) 1.
14. S.P. Jiang, J.P. Zhang, Y. Ramprakash, D. Milosevic and K. Wilshier, *J. Mater. Sci.* **35** (2000) 2735.
15. S.H. Chan, K.A. Khor and X.J. Chen, *J. Electrochem. Soc.*, in press.
16. Y.J. Leng, S.H. Chan, K.A. Khor, S.P. Jiang and P. Cheang, *J. Power Sources* **117** (2003) 26.
17. J.P. Zhang, S.P. Jiang, J.G. Love, K. Foger and S.P.S. Badwal, *J. Mater. Chem.* **8** (1998) 2787.
18. E.P. Murry and S.A. Barnett, *Solid State Ionics* **143** (2001) 265.
19. T. Kenjo and M. Nishiya, *Solid State Ionics* **57** (1992) 295.
20. J.A.M. van Roosmalen and E.H.P. Cordfunke, *Solid State Ionics* **52** (1992) 303.
21. S.P. Jiang and J.G. Love, *Solid State Ionics* **138** (2001) 183.
22. S.P. Jiang, J.P. Zhang and K. Foger, *J. Electrochem. Soc.* **147** (2000) 3195.
23. A. Mitterdorfer and L.J. Gauckler, *Solid State Ionics* **111** (1998) 185.
24. S.P. Jiang and J.G. Love, *Solid State Ionics* **158** (2003) 45.
25. H.Y. Lee, W.S. Cho, S.M. Oh, H-D. Wiemhöfer and W. Göpel, *J. Electrochem. Soc.* **142** (1995) 2659.
26. J. Winkler, P.V. Hendriksen, N. Bonanos and M. Mogensen, *J. Electrochem. Soc.* **145** (1998) 1184.